PHYSICAL REVIEW B VOLUME 18, NUMBER 10 15 NOVEMBER, 1978

Experimental energy dispersions for valence and conduction bands of palladium

F. J. Himpsel and D. E. Eastman
IBM Thomas J. Watson Research Center, Yorktown Heights, New York 10598
(Received 15 June 1978)

Using angle-resolved photoemission with synchrotron radiation, we have determined accurate energy-versus-momentum dispersion relations along the $\langle 111 \rangle$ direction using a Pd(111) crystal. The energy E ($\lesssim 0.1$ eV accuracy) and the momentum parallel to the surface $\vec{k}_{\parallel}$ are measured directly. The perpendicular component of the momentum $k_{\perp}$ is obtained from the measured final energy via a calculated free-electron-like final band that is found to be accurate within $\pm 5\%$ of the zone-boundary momentum by comparison with certain critical points that have been measured directly (L_1, Γ'_2, and Γ_{15}). For the initial bands, we find the dispersions of the two d-like Λ_3 bands and of the sp-type Λ_1 band. Measured critical points (in eV) for bands numbered with increasing energy are: $\Gamma_{2,3,4} = -2.55 \pm 0.15$, $\Gamma_{5,6} = -1.15 \pm 0.1$, $\Gamma_7 = 18.4 \pm 0.5$, $\Gamma_8 = 21.7 \pm 0.5$, $L_4 = -0.4 \pm 0.2$, $L_5 - 0.1 \pm 0.1$, and $L_7 = 7.7 \pm 0.3$. Spin-orbit splitting (~ 0.4 eV maximum) is observed for the upper Λ_3 band.

INTRODUCTION

The main studies of the electronic structure of clean Pd surfaces and bulk Pd have been band calculations.[1-5] So far, the most detailed experimental information is given by de Haas–van Alphen Fermi-surface data.[6,7] For energies away from the Fermi level, only very indirect information about electronic states has been gathered by optical[8] and angle-integrated photoemission experiments.[9-11]

Our angle-resolved photoemission data permit a direct determination of E vs $\vec{k}$ dispersions for the occupied bands, and give critical points of the empty bands up to more than 20 eV above the Fermi level E_F. This makes a critical review of different Pd band-structure calculations possible, and improves the basis for more refined Pd calculations as well as for surface-chemisorption and bulk hydride calculations.

Our method to determine energy bands experimentally has been tested previously for[12] Cu and Ni,[13] where a wealth of very specific optical and angle-resolved photoemission data exist. It consists of two steps: First, information about critical points of final bands is collected. Conduction-band critical points can be seen either as structures in the angle-resolved spectrum of secondary electrons, or can be derived from extremal behavior of interband intensities.[14] Once the key critical points are known for the final bands, a band-structure calculation is used to interpolate between these points. Such semiempirical final bands are used to obtain the component of the momentum perpendicular to the surface, $k_{\perp}$, from the measured final energy of photoelectrons. The reduced momentum parallel to the surface $\vec{k}_{\parallel}$, is measured directly since it is conserved during the photoemission process for a smooth single crystal. The initial-state energy and momentum are obtained from the final energy and momentum by subtracting the photon energy $h\nu$ and photon momentum (the latter is negligible in our case). Errors in the final-energy bands are demagnified for the initial bands by the ratio of the slopes of the bands in question, typically by a factor of 5. This makes our method rather accurate for occupied bands. Typical uncertainties are less than 0.2 eV and ±5% of the zone-boundary momentum, respectively.

EXPERIMENTAL

The data were taken with a new two-dimensional display-type spectrometer at the 240-MeV electron storage ring of the University of Wisconsin. It combines an elliptical reflection-mirror low-pass filter with a retarding-grid high-pass filter to achieve a band pass energy analyzer while accepting a full 86° cone of emission angles (1.8 sr). An angle-resolving detector selects electrons emitted within a 4°-full-angle cone. Reducing the angular acceptance to 2° full angle did not change the energy distribution curves. The overall energy resolution of the system (photons and electrons) was 120 meV in this experiment, with typical count rates of 10^4 sec in the Pd d bands. A Pd(111) surface was prepared by ion etching and subsequent annealing (~600 °C) and recleaned by mild heating ($\lesssim$500 °C) after about 0.5 h in a working vacuum in the 10^{-11}-Torr range. Auger electron spectroscopy and low-energy electron diffraction were used to characterize the surface.

RESULTS AND DISCUSSION

Figure 1 shows angle-resolved energy distribution curves (AREDC's) for photoelectrons emitted

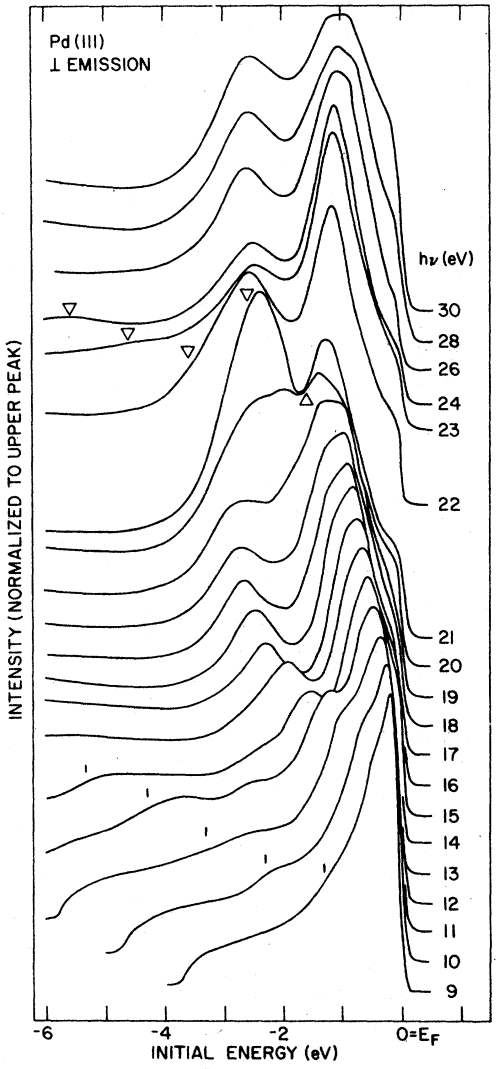

FIG. 1. Angle-resolved photoelectron energy distributions for normal emission from Pd(111) at different photon energies $h\nu$. Light was entering in the $(\bar{1}1\bar{2})$ plane at 59° from normal with the $\vec{E}$ vector in the plane of incidence. Curves have been offset for different $h\nu$ and are normalized to the upper peak.

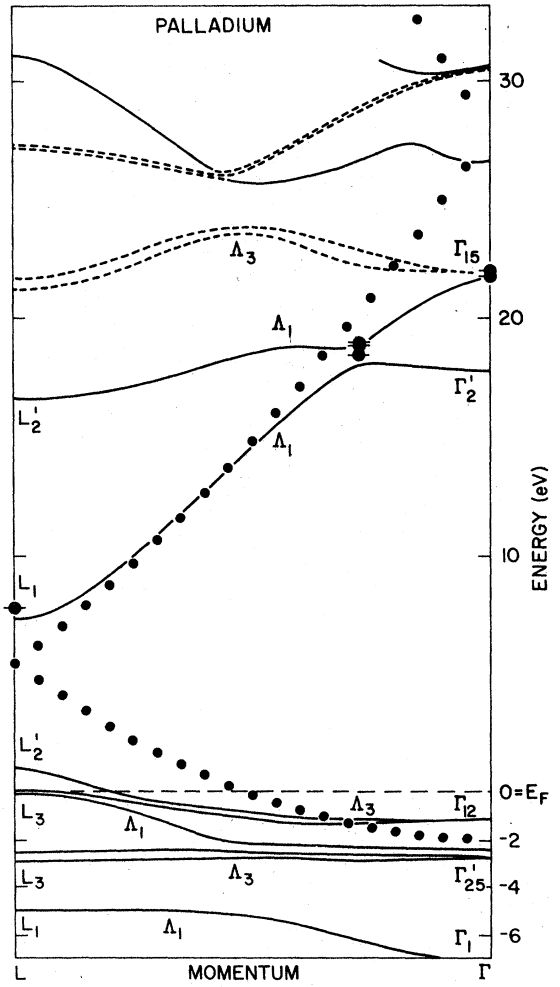

FIG. 2. Band structure of palladium after Christensen. Dashed lines are Λ_3 final bands not seen in normal emission. The dotted line is a free-electron parabola shifted by an inner potential. Fat dots with crossbars are conduction-band points determined from our data.

normal to the Pd(111) surface. AREDC's for different photon energies $h\nu$ are displaced vertically. As general features, we note: (i) A maximum at ~−1 eV initial energy that is split by up to 0.4 eV for certain $h\nu$'s. This is attributed to direct transitions from the spin-orbit-split upper Λ_3 d band into the free-electron-like Λ_1 final band (see Fig. 2). (ii) A smaller peak appearing at $h\nu \sim 9$ eV on the low-energy tail of maximum (i) and dispersing towards lower initial energies for increasing $h\nu$. This is due to direct transitions from the Λ_1 sp band into the free-electron-like Λ_1 final band. (iii) A shoulder at ~−2.5 eV initial energy (low $h\nu$) that shows a strong intensity maximum at $h\nu \sim 21$ eV where it is resonant with structure (iv). We assign the shoulder to direct transitions from the lower Λ_3 d band into the Λ_1 free-electron-like final band and the resonance to excitations from the same initial band into a flat f-like Λ_1 final band. (iv) A weak enhancement of the secondary electrons (~7%; sensitive to contamination) at 18.4 eV final energy [full width at half-maximum FWHM of ~1 eV], marked by triangles in Fig. 1. This is associated with a flat f-like Λ_1 final band connected to Γ_2' and L_2'. (v) A steplike structure in the secondary electron energy distribution at 7.7-eV final energy (turning point), which is also independent of $h\nu$. This marks the bottom of the free-electron-like Λ_1 final band (L_1) since the effective sampling depth is substantially smaller

for evanescent states in the band gap below L_1.

Also, additional information about final band critical points can be extracted from the intensity and splitting of structure (i). The intensity of peak (i) [normalized to the incident photon flux (not shown in Fig. 1)] reaches a maximum at $h\nu = 22.8$ eV. At the same photon energy the splitting disappears. This indicates that the transition takes place at Γ and places the final Γ point at 21.7 eV above E_F, which is very close to the calculated Γ_{15} point. Peak (i) shows a shallow intensity minimum at $h\nu = 20$ eV. This corresponds to a final energy of 18.9 eV, which is close to the energy position of the flat f-like Λ_1 band as determined independently from the resonance behavior of structure (iii) at 18.8-eV final energy and from structure (iv) at 18.4-eV final energy. It appears that the uppermost occupied Λ_3 band (i) has a large transition-matrix element to the free-electron-like Λ_1 conduction band, and is therefore attenuated in the small gap induced by the interaction of this final band with the f-like flat Λ_1 final band. On the other hand, the lower occupied Λ_3 band (ii) couples more strongly to the f-like final band than to the nearly-free-electron final band.

The experimental conduction-band features discussed above are summarized in Fig. 2 (dots with horizontal dash) and compared to Christensen's[4] calculation, which is expected to be the most reliable one for high conduction bands. The deviations between theory and experiment are typically 0.5 eV, which is comparable to the uncertainty in localizing the higher-energy conduction-band features experimentally. Therefore, we use Christensen's final bands without modification to determine our initial bands. A free-electron final band (with an adjusted inner potential) is clearly not accurate enough to represent final bands in Pd (see Fig. 2, dotted line).

In Fig. 3 we present our experimental energy dispersions for the initial bands along the $\Gamma\Lambda L$ line. The dots correspond to direct transition structures in Fig. 1. The initial energy is obtained by subtracting $h\nu$ from the measured final energy ($\lesssim 0.1$–0.2 eV accuracy). The value of $k_\perp$ along the $\Gamma\Lambda L$ line is obtained from the measured final energy as well, using the conversion scale given on top of Fig. 3 which in turn corresponds to Christensen's final bands (Fig. 2). Full circles refer to the first final band and open circles refer to the second.

To compare with different calculations and experiments, energy values for critical points have been collected in Table I. Since there is no unique symmetry assignment from different relativistic calculations, we have numbered the bands with increasing energy. Approximate nonrelativistic

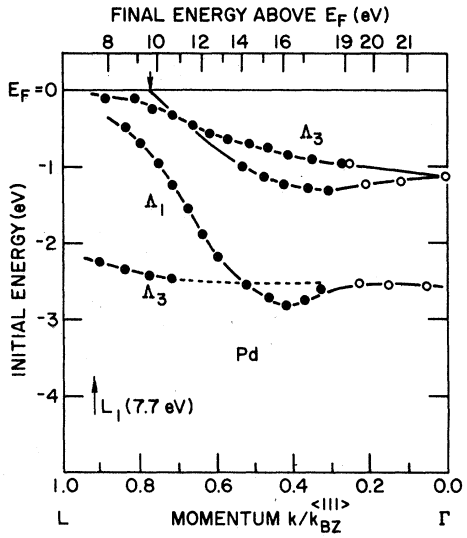

FIG. 3. Experimental E vs $\vec{k}$ energy band dispersions for Pd along Λ. The energy scale on top of the figure refers to the conversion of the observed final energy into the momentum using the bands shown in Fig. 2.

labels are given in Fig. 2. Generally, there is good agreement between experiment and theory. Two characteristic deviations at an accuracy level of $\lesssim 0.2$ eV should be noted. Relativistic *ab initio* calculations[2,4] as well as relativistic interpolation schemes[1,3] yield a small Γ-centered fifth-band hole pocket.

In our data ($h\nu \sim 9$ eV) the direct transitions from the fifth band are still seen at L. de Haas–van Alphen experiments[6,7] could not find a corresponding hole pocket at L either, which led to the conclusion that there is no such hole pocket. Second, our observed spin orbit splitting of the upper Λ_3 band (0.3–0.4 eV) is substantially larger than calculated (typically 0.2 eV) and closer to the atomic spin orbit splitting of 0.44 eV.[15] The experimental value is an upper limit for the spin orbit splitting, since extra crystal-field splitting is seen for states off the Λ axis. Those could be sampled via k transfer from surface imperfections.

Accurate comparisons with other experimental results are hardly possible due to the lack of detailed information. The value for the L_7 point (7th band, Table I) obtained by Traum and Smith[10] from angle-integrated photoemission with clean and cesiated polycrystalline samples agrees well with our result. Optical data[8] has not been successfully used to derive band-structure information in Pd,[4] except for one recent thermomodulation experiment[16] that shows the strongest feature at the same photon energy ($h\nu \sim 21$ eV), where we see resonant enhancement of transitions from the lower Λ_3 d band caused by a f-like flat final band.

TABLE I. Experimental and *ab initio* calculated energy values for special points on the $\Gamma\,\Delta L$ axis in palladium (in eV relative to E_F).

$\vec{K}$ point, band number	This experiment	Other experiments Ref. (10)	Andersen Ref. (2) Christensen Ref. (4) RAPW [a]	Mueller *et al* Ref. (1) $4d^{10}$ HFS [b]	Louie Ref. (5) self-consistent pseudopotential
$\Gamma 2,3,4$	-2.55 ± 0.15		-2.79	-2.59	-2.56
			-2.49		
$L\,2,3$	$-2.4\ \pm0.2$		-2.98	-2.70	-2.66
			-2.62		
$\Gamma 5,6$	-1.15 ± 0.1		-1.17	-1.19	-1.21
$L\,4$	$-0.4\ \pm0.2$		-0.14	-0.06	-0.09
$L\,5$	$-0.1\ \pm0.1$		$+0.05$	-0.06	-0.09
$L\,7$	$+7.7\ \pm0.3$	$+8.0\pm0.2$	$+7.30$		
$\Gamma 7$	$+18.4\ \pm0.5$		$+17.71$		
$\Gamma 8$	$+21.7\ \pm0.5$		$+21.65$		

[a] RAPW: relativistic augmented plane wave.
[b] $4d^{10}$ HFS: Hartree-Fock-Slater potential for the $4d^{10}$ configuration.

To summarize, we have determined for the first time experimental energy-band dispersions for Pd. Our results can be used together with an interpolation scheme to give a more accurate theoretical description of Pd, as well as a basis for future calculations of more complex Pd-adsorbate or Pd-H systems.

ACKNOWLEDGMENT

We wish to acknowledge the excellent support of the Synchrotron Radiation Center Wisconsin, and the many contributions of J. A. Knapp, J. J. Donelon and, A. Marx. This research was supported in part by the AFOSR under contract No. F44620-76-C-0041.

[1] F. M. Mueller, A. J. Freeman, J. O. Dimmock, and A. M. Furdyna, Phys. Rev. B 1, 4617 (1970).
[2] O. K. Andersen, Phys. Rev. B 2, 883 (1970).
[3] N. V. Smith and L. F. Mattheiss, Phys. Rev. B 9, 1341 (1974).
[4] N. E. Christensen, Phys. Rev. B 14, 3446 (1976).
[5] S. G. Louie, Phys. Rev. Lett. 40, 1525 (1978).
[6] L. R. Windmiller, J. B. Ketterson, and S. Hornfeldt, Phys. Rev. B 3, 4213 (1971).
[7] D. H. Dye, G. W. Crabtree, J. B. Ketterson, J. J. Vuillenium, and N. B. Sandesara, Bull. Am. Phys. Soc. 23, 208 (1978).
[8] J. H. Weaver, Phys. Rev. B 11, 1416 (1975).
[9] J. F. Janak, D. E. Eastman, and A. R. Williams, Solid State Commun. 8, 271 (1970).
[10] M. M. Traum and N. V. Smith, Phys. Rev. B 9, 1353 (1974).
[11] H. Höchst, S. Hüfner, and A. Goldmann, Phys. Lett. A 57, 265 (1976).
[12] J. A. Knapp, F. J. Himpsel, and D. E. Eastman (unpublished).
[13] F. J. Himpsel, J. A. Knapp, and D. E. Eastman (unpublished).
[14] E. Dietz *et al.* (unpublished).
[15] C. E. Moore, *Atomic Energy Levels*, U. S. Natl. Bur. Stand. Circ. No. 467 (U. S. GPO, Washington, D. C., 1958).
[16] C. Olson (private communication).